

# Green synthesis of ZnO nanoparticles using *Moringa oleifera* leaf extract for efficient photocatalytic degradation of organic dyes

Ganesan D.<sup>1</sup>, Lakshmanaprabhu S.<sup>2\*</sup>, Priyadharsini K.<sup>3</sup> and Hemavathi<sup>4</sup>

<sup>1</sup>Department of Civil Engineering, Mahath Amma Institute of Engineering and Technology, Pudukkottai-622101, Tamil Nadu, India

<sup>2</sup>Department of Pharmaceutical Technology, Bharathidasan Institute of Technology, Anna University, Tiruchirappalli-621316, Tamil Nadu, India

<sup>3</sup>Department of Physics, Tagore Engineering College, Chennai-600127, Tamil Nadu, India

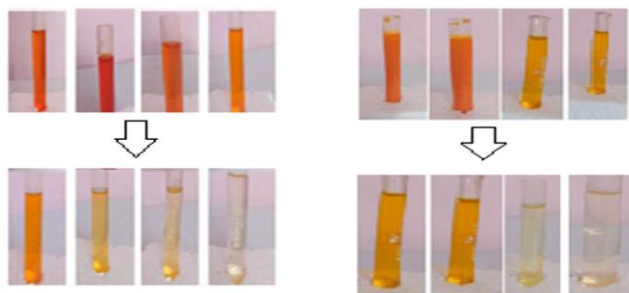
<sup>4</sup>Department of Civil Engineering, K Ramakrishnan College of Technology, Trichy-621112, Tamil Nadu, India

Received: 29/09/2023, Accepted: 01/11/2023, Available online: 07/11/2023

\*to whom all correspondence should be addressed: e-mail:

<https://doi.org/10.30955/gnj.005411>

## Graphical abstract



## Abstract

In this research, we provide a method for synthesizing ZnO nanoparticles using *Moringa Oleifera* Leaf (M.O Leaf) Extract. UV-VIS Spectroscopy, Scanning Electron Microscopy, EDS, X-ray diffraction and Fourier Transform Infrared Spectroscopy (FTIR) were used to create and characterize ZnO nanoparticles. The spherical size structure of the synthesized nanoparticles with an average grain size of 1 nm was validated by SEM, EXD, and XRD analysis. After the sunlight exposure, the photocatalytic reagent was used to break down the organic dyes in the synthesized ZnO nanoparticles. Nearly 96–97% of the titan yellow and Congo Red dyes were broken down by ZnO nanoparticles.

**Keywords:** Biosynthesis, M.O Extract, ZnO nanoparticles, dye degradation.

## 1. Introduction

Nanotechnology has sparked a great deal of curiosity in the present period of scientific research in all fields. Nanoparticles (NPs) are fundamental nanotechnology components and serve as its foundation. Nanoscience and nanotechnology are now widely used in various sectors, primarily in applications for sensors, electronic devices, antibacterial agents, water purification, cosmetics, biopharmaceuticals, environmental protection, catalysis, and materials. The nonmaterial's catalytic, magnetic,

electrical, and optical characteristics can be significantly influenced by their size, crystallinity, and shape (Sharma *et al.* 2019). The primary benefits of creating nanoparticles at room temperature and using plant extracts are that they help to partially complete a green synthesis (Gopinath *et al.* 2012; Singh *et al.* 2017). Physical, biological, chemical, and recently green methods create metal and metal oxide nanoparticles. Zinc oxide and ZnONPs have a significant role and are excellent semiconductors. In nature, there is a wide variety of band gaps (3.37) with high excitation binding energies (60 meV) that depend on ambient temperature (El-Rafie *et al.* 2012). Excellent thermal and chemical stability and remarkable optical behaviour are characteristics of zinc oxide and ZnONPs (Bhuyar and Ganesan 2017). The biosynthesis of various nanoparticles and photodegradation properties are currently of great interest. Recent research has documented the significant photo-degradation effects of various metal and metal oxide nanoparticles when exposed to visible light irradiation (Rajiv *et al.* 2013). Various plant extracts serve as the primary raw material for the environmentally friendly large-scale synthesis of NPs, including the production of Au, Ag, and Pd, among other noble metal nanoparticles. Extracts from various plant components, including geranium leaves, lemongrass, and neem leaves, along with compounds like Aloe vera, have been utilized for this purpose (Sathishkumar *et al.* 2009; Vijayakumar *et al.* 2015; Suman *et al.* 2015; Khatoon and Mollah 2016; Rajkumari *et al.* 2017). This article also highlights significant applications of ZnONPs in both environmental and biological domains. These applications span various areas, including delivery of drugs, sensing of biological elements and labelling, transport of genes and nanomedicine (Shankar *et al.* 2004; Saifuddin *et al.* 2009; Mittal *et al.* 2013; Bindhu and Umadevi 2013). Moreover, it delves into patents associated with ZnONPs, covering against the diabetic, fungal, bacterial and pre-adulticidal activities (Bar *et al.* 2009; Nanda and Saravanan 2009; Rathi *et al.* 2016; Sudhakar *et al.* 2016; Ahmed and Ikram 2016).

Numerous therapeutic plants and extracts obtained from their leaves and calyxes have demonstrated notable qualities such as dilution of drugs antioxidant, lowering the BP, chemical protection, and hypotensive against tumour and cancer action (Nadagouda and Varma 2008; Das *et al.* 2009; Geethalakshmi and Sarada 2010; Rajakumar and Rahuman 2011; Oves *et al.* 2013). In the textile industry, various organic colour dyes have been extensively used, resulting in the generation of a considerable amount of wastewater containing toxic and vibrant dyestuffs during manufacturing. This has led to the pollution of surface and groundwater. Various physical and chemical processes have been employed to address this issue to remove these hazardous contaminants. These processes include electrocoagulation (Jha *et al.* 2009), flocculation/coagulation (Huang *et al.* 2007), and carbon adsorption (Shukla *et al.* 2019). Mahendra and Vinay (2014) showed that ZnONPs exhibit antibacterial activity against Gram-positive and Gram-negative microorganisms. Banerjee *et al.* (2014) used zinc acetate dihydrate to manufacture ZnO nanowires by a hydro-thermal process at 90°C. Azizi *et al.* (2014) biosynthesized silver nanoparticles with antibacterial properties using mine soil microbes as a natural precursor. This study used *Moringa oleifera* leaves as a natural precursor to create ZnONPs. The nanoparticles created were around 52 nm and were characterised using various methods. We also assessed the synthesized ZnO nanoparticles' antibacterial activity against Gram-positive and Gram-negative bacteria. In addition, we assessed the photocatalytic activity using the organic dye titan yellow, which was chosen as a representative dye in our study.

## 2. Experimental and materials

### 2.1. Gathering of samples

*Moringa Oleifera* leaves were collected in the vicinity of Pudukkottai. These leaves were soaked and left to air dry at room temperature naturally.

### 2.2. Extracting leaves from *Moringa oleifera*

The *Moringa oleifera* leaf was taken from a nearby field in Tamil Nadu's Pudukkottai. 20g of freshly harvested *moringa oleifera* leaves were finely chopped and cleaned with distilled water, as shown in Figure 1. Using a mixer grinder, the dried leaves were ground into powder and boiled for 1 hour at 60 degrees Celsius with 100 ml of double-distilled water. The mixture was boiled, cooled, and filtered through Whatman No. 1 filter paper; the filtrate was then collected in Liquid Figure 2 (a and b).



**Figure 1.** *Moringa Oleifera* Leaf



**Figure 2.** (a) M.O Leaf Powder Boiling (b) M.O Leaf Extract Liquid

### 2.3. Zinc oxide nanoparticle synthesis

In order to create zinc oxide nanoparticles using a precipitation reaction method, 50 ml of 20% NaOH solution and 10 ml of *Moringa Oleifera* leaf extract were combined. After that, a 250 ml beaker was filled with a 5 ml solution of this combination and 50 ml of distilled water, and the mixture was stirred for 1 hour. Then, dropwise additions of zinc acetate (2.1g in 100ml water) and ammonium carbonate (0.96g in 100ml) solutions were made while the beaker was continuously stirred. The suspension continued swirling at 750 rpm for one hour at a temperature of 24°C after the reaction. The precipitate was filtered and repeatedly washed with ethanol and an ammonia solution. The resulting precipitates were subsequently subjected to vacuum drying for 12 hours. Following this, they were placed up to 5 hours in the muffle furnace at 350°C. This process resulted in the production of zinc oxide nanoparticles, which were subsequently collected and stored in a vacuum-sealed container for future use (Figure 3).

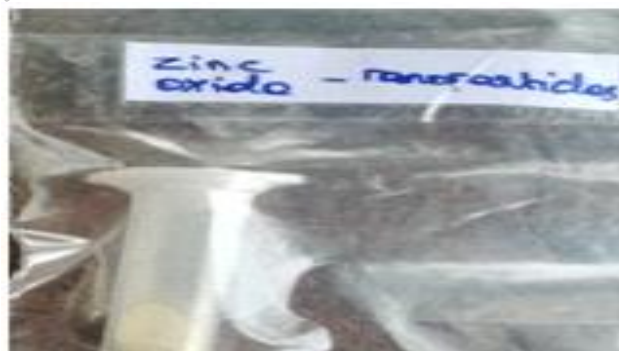


**Figure 3.** ZnO-NPs nano particles

### 2.4. ZnO nanoparticles physicochemical characterization

At 350–400 nm wavelength, a UV–visible spectrophotometer (Perkin Elmer Lambda 35) was used to characterize the synthesized ZnO–NPs. Using the Perkin Elmer FTIR-ATR spectrometer (LI60300 spectrum two Lita SN 96499) with a KBr pellet, the functional groups existing in the synthesized ZnONPs were examined with a spectrum range of 4000-400  $\text{cm}^{-1}$ . The SEM (Scanning Electron Microscope) and XRD (X-ray Diffraction) analyses were performed to analyze the surface morphology and crystalline structure of the synthesized ZnONPs. We conducted X-ray diffraction (XRD) analysis in the range of 10 to 80 degrees using a CuK target and Ni-filter with a Benchtop PROTO AXRD X-ray diffraction analyzer. Scanning electron microscope (SEM) images were also generated using a 15 KV scanning electron microscope.

### 2.5. Nanoparticle photocatalytic activity in visible light

Under the natural sunlight with synthesized ZnONPs, the titan dye solution and its photocatalytic degradation were assessed in fixed experimental conditions. The Congo red & Tital yellow dyes were taken 100 ml each (1.2M – 4M), and 100 mg of synthesized ZnONPs was added into that dye solution. Then, the final suspension was taken in a 250 ml conical flask and placed on the magnetic stirrer. The final suspension was kept in an ideal state for 10 minutes to attain the equilibrium. At regular intervals of 10 minutes, 5ml reaction mixtures were obtained, and the solution was centrifuged for measurement. The suspension mixture's absorption spectrum was periodically monitored using a UV-visible spectrophotometer. Lastly, the reaction mixture's change in colour from coloured to colourless indicated that the degradation process was finished in one hand and the dye degradation using Equation 1.

$$\% \text{ degradation} = \frac{A_0 - A_t}{A_0} \times 100 \quad (1)$$

where  $A_0$  is the absorbance of dye during the earlier stage, and  $A_t$  is the absorbance of dye at any time  $t$ .

### 2.6. Antimicrobial activity in vitro

The Agar Cup Method (Verma and Sharma 2016) was used to examine the ZnONPs' antibacterial activity in qualitative antimicrobial screening. *Bacillus subtilis* and *E. coli* were used as two test microorganisms for this investigation. This method was employed with even swabbing *E. coli* and *Bacillus subtilis* on the nutritional agar medium with germ-free cotton. Sterilized Nutrient Agar Plates were then made. The surface of the nutritional agar plates was then prepared with the aid of the Cork Borer. The nutrient agar plates were placed in an incubator at 37°C for 24 hours, along with the synthesized ZnO nanoparticles in the wells. After the specified incubation period, the plates were inspected for the presence of zones, and these zones were measured in centimetres (cm). They were then presented as clear areas surrounding the wells.

## 3. Results and discussion

In the current study, it is described how dried leaves can be used to create nanoparticles without the use of external accelerating or stabilizing substances and the need for constant stirring. A white precipitate indicates that zinc oxide nanoparticles (ZnONPs) were formed in the mixture.

### 3.1. UV-visible spectra analysis

The synthesized ZnONPs absorption spectra are depicted in Figure 4 and Table 1, with an absorption peak at about 361 nm. Because ZnONPs have a high excitation binding energy at ambient temperature, it suggests that they exhibit excitation absorption (at 361 nm). The existence of distinct bands in the zinc colloids at 361 nm demonstrates that the *Moringa Oleifera* leaf extract effectively reduces zinc ions. The wavelength of this absorption peak at 361 nm signifies the existence of a blue-shifted absorption spectrum compared to the bulk value of ZnONPs, typically at 377 nm. This finding is consistent with prior research (Shankar *et al.* 2004).

**Table 1.** UV-Visible Spectra Peaks for ZnONPs

Name	No.	Peak(nm)	Peak (AU)
Zinc-Oxi-NP	1	277.40	1.695
	2	298.45	1.696
	3	324.45	1.723
	4	361.65	2.200

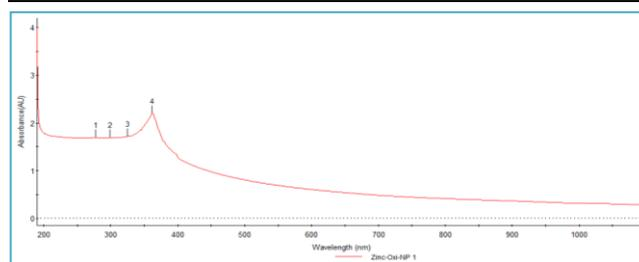


**Figure 4.** UV-Visible Spectra Analysis of ZnONPs

### 3.2. FT-IR Analysis

The probable biomolecules in *Moringa Oleifera* leaf extract that are in charge of capping and effectively stabilizing ZnO nanoparticles were determined using FTIR measurement (Figure 5), which is consistent with past research (Kim *et al.* 2009; Suresh *et al.* 2015). For metal-oxygen bonds, the range between 400 and 4000  $\text{cm}^{-1}$  is designated. The presence of ZnONPs is indicated by the absorption peak at 3436.14  $\text{cm}^{-1}$ , along with absorption bands corresponding to the biomolecules used for decrease and equilibrium (capping agents) at wavelengths of 3436.14, 2922.74, 1638.06, 1413.43, 1030.12, 856.53, and 543.16 (Basnet *et al.* 2015).

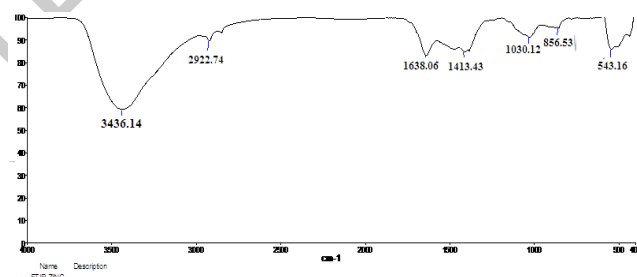


**Figure 5.** FT-IR Analysis of ZnONPs

### 3.3. XRD analysis

All of the diffraction peaks of synthesized ZnONPs match those of normal ZnOPs, according to the XRD patterns of these materials. The diffraction peaks shown in Figure 6 of the XRD analysis closely correspond to the hexagonal quartzite structure, as confirmed by the data from JCPDS card No. 89-1397 (Vivek *et al.* 2012). The samples are highly crystalline, as seen by the peaks in (Figure 6 (A)), which are both sharp and strong. For diffractions from the (1 0 0), (0 0 2), (1 0 1), (1 0 2), (1 1 0), (1 0 3), (2 0 0), (1 1 2), and (2 0 1) planes, the pattern can be indexed. The XRD analysis indicates the remarkable purity of the derived products, as there are no additional diffraction peaks related to impurities. The nanometer range crystalline structures were observed based on the observations of broad peaks. Equation 2 can calculate the size (D) of crystalline structures.

$$D = \frac{K\lambda}{\beta \cos \theta} \quad (2)$$

K represents the constant of the Scherrer equation,  $\lambda$  represents the wavelength,  $\beta$  represents the half maximum peak, and  $\theta$  represents the diffraction angle (Arvizo *et al.* 2012). XRD data was used to estimate the average zinc oxide crystallite size, which was 52 nm.

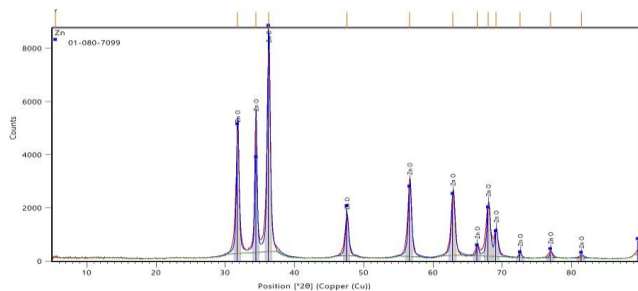


Figure 6. XRD Analysis of ZnONPs

### 3.4. SEM Evaluation

After verifying the XRD results, the sample was further processed for the SEM analysis. Figure 7 shows an SEM image demonstrating the ZnONPs size, shape, and surface morphology. The synthetic products' spherical, crystalline structure and around 52nm diameter are shown by thorough structural characterizations.

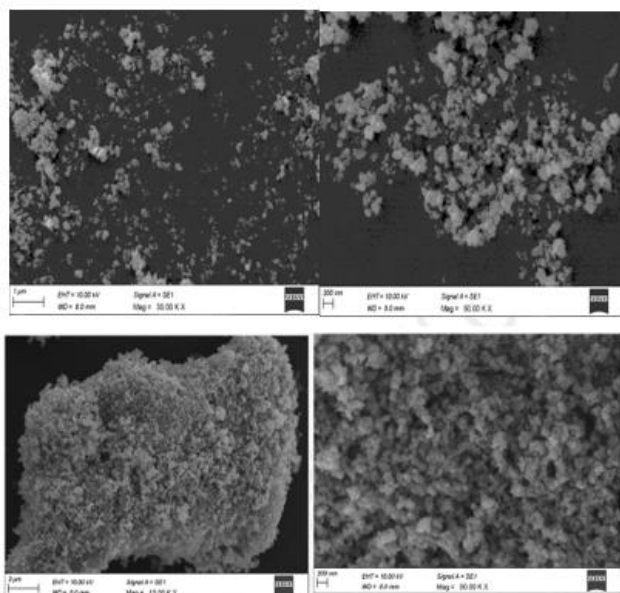


Figure 7. SEM Analysis of ZnONPs

### 3.5. EDX analysis of ZnONPs

The EDX spectra of ZnONPs created at room temperature are shown in Figure 8 to demonstrate further the zinc atoms' presence in the zinc nanoparticles. The graph produced by the EDX analysis shows the zinc elements to be present. The weight percentage of zinc in ZnONPs decreased by M.O Leaf by 84.09%. Table 2 Elemental components existed sample of zinc nanoparticles (EDX). This shows that zinc oxide has been reduced to zinc elements. The optical absorption peak, typical for the absorption of zinc nano crystallites due to SPR, was seen at 2.6, 2.8, 3, and 3.2 keV. This demonstrated that zinc was one of the elements. Individual, spherical zinc nanoparticles produced with Triam, the made candra in a prior study, displayed absorption peaks in the 2.8 to 3.8 keV region, which is identical to consistent with the outcome obtained when M.O leaf was used as the reducing agent.

The EDX examination reveals the oxygen's feeble signal. Zinc signals and oxygen peak point to biomolecules in the plant extract.

Table 2. Elemental components existed sample of ZnONPs

Nos	Element	Weight %	Atomic %	Error %
1	O K	15.91	43.59	7.19
2	Zn L	84.09	56.41	2.8

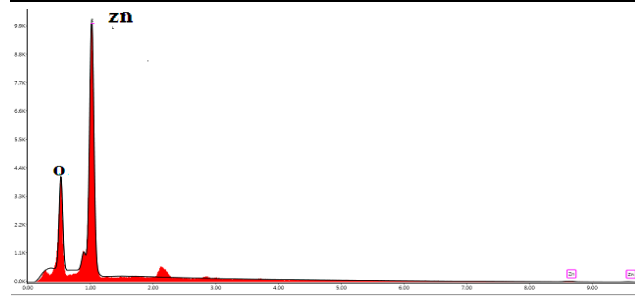


Figure 8. EDS Analysis of ZnONPs

### 3.6. Size and potential of the zeta

According to some theories, the stability of nanoparticles is significantly influenced by zeta potential. The zeta potential of green synthesized ZnONPs (Figure 8) was found to be 121.1 (d. nm) zeta Average with 119.7 size (d. nm) and intensity (99%), demonstrating that the surface of the nanoparticles was positively excellent quality charged that dispersed in the good.

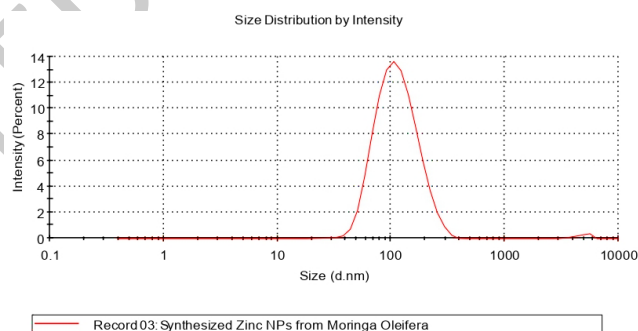


Figure 8. Zeta Potential of ZnONPs

### 3.7. ZnONP photocatalytic activity in visible light

Figure 9 depicts the photo-catalytic degradation of titan yellow and Congo red dyes over various time intervals utilizing green synthesized ZnONPs. Figure 10 is an aromatic heterocyclic chemical compound, titan yellow. The spectra of Congo Red and Titan Yellow solutions in an aqueous medium are displayed in Figures 9 and 10, respectively, revealing characteristic peaks at 226, 321, and 407 nm. The decrease in absorbance at 407 nm over time in the presence of visible light illumination, after exposure to ZnONPs suspension is likely attributed to the degradation of the chromophores.

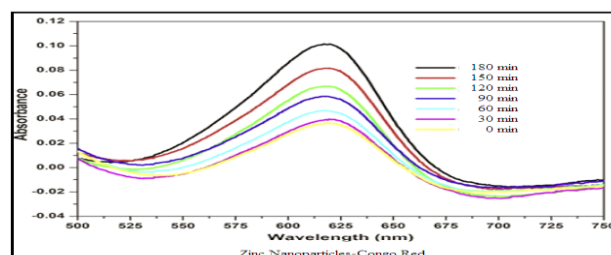


Figure 9. ZnONPs vs. Congo Red Photocatalytic

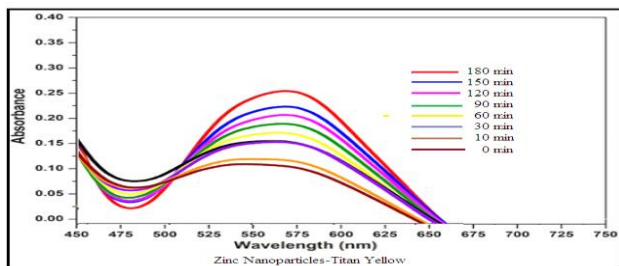


Figure 10. ZnONPs vs. Titanium yellow Photocatalytic

### 3.8. Result of pH

Since pH plays many functions in the dye photo-degradation process, interpreting its effects on effectiveness is challenging. Therefore, it is essential to consider how pH affects the rate of deterioration. Zinc was used in experiments with pH ranges of (2.1–10) as shown in Table 3. With rising pH, photocatalysis was more prevalent. This unequivocally proves that zinc would dissolve in an acidic environment. More hydroxyl anions were present at higher pH levels, which aided in the photogeneration of hydroxyl radicals.

Table 3. Variation of pH Vs Time

Time (mins)	pH	Temp (°C)
0	6.2	30
10	4.8	
30	5.3	
60	3.9	
90	2.8	
120	2.1	
150	8.2	
180	10	

### 3.9. Impact of light intensity

The impact of light intensity on photo-degradation efficiency has been studied at constant dye concentration and nanoparticle loading. It is obvious that as light intensity rises, photodegradation and decolorization percentages also rise. The energy of a photon is linked to its wavelength, and the overall energy supplied to a photocatalytic process relies on light intensity. Ultraviolet (UV) irradiation generates the photons needed to transfer electrons from the valence band to the conduction band of a semiconductor photocatalyst. As more radiation strikes the catalyst surface and produces more hydroxyl radicals, the rate of deterioration rises.

### 3.10. Temperature effect

It has been established that temperature plays a significant role in the photocatalysis of dyes. In the UV/metal nanoparticles method, nanoparticles' photocatalytic degradation rate as a temperature function was investigated. Under 30°C, the photocatalytic activity of zinc, silver, and iron nanoparticles was more effective. The photocatalytic properties of the synthesized ZnONPs are widely recognized and influenced by several factors, including size, shape, surface area, and the electronic state of the metal. Without a photocatalyst, the self-degradation of Congo Red and Titan Yellow dye in visible light was limited. However, in the presence of our synthesized nanoparticles, approximately 97% and 96% degradation of

the dyes occurred, respectively. The importance of particle sizes has already been reported. The photocatalytic activity diminishes due to a decrease in surface area caused by temperature (Firdhouse and Lalitha 2015). The reductions in Congo's absorbance and the presence of ZnONPs in red dye and titan yellow dye solution demonstrated the substantial photodegradation capacity of the synthesized nanoparticles. Figure 7 illustrates how the deterioration efficiency rises over time. Table 1 compares the degradation (97% and 96%) of various dyes when ZnONPs are used, depending on the pH range of the dye solution. We can infer from the table that our synthesized nanoparticles exhibit outstanding degradation over a wide time range. Figure 1 (inner image) depicts the dye solution's colour change.

### 3.11. Activity against microorganisms

Gramme positive and gramme negative bacteria were used to examine the ZnO nanoparticles' anti-bacterial activities. Table 4 and Figure 11 summarise the results, demonstrating that ZnO nanoparticles exhibit potent antibacterial activity against Gram-positive and Gram-negative microorganisms, including *Bacillus subtilis* and *E. coli*. The results of the experiments unmistakably point to the nanoparticles' potent growth-inhibitory activity against microorganisms and their robust association with *Bacillus subtilis* and *E. coli*.

Table 4. ZnONP inhibitory zone diameters (cm) against bacterial species

Sample	Inhibition region	
	<i>Bacillus subtilis</i>	<i>Escherichia coli</i>
ZnONPs	3.5 cm	3.3cm

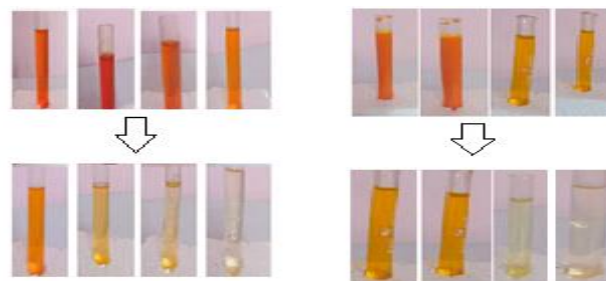


Figure 11. Efficiency of colour change due to decomposition of Congo Red (left) and Titan Yellow (Right)

## 4. Conclusion

This study used *Moringa Oleifera* leaf extract as a natural precursor to create ZnO-NPs utilizing a relatively straightforward and practical precipitation approach. The fundamental benefit of this synthesis is its straightforward and economical synthetic approach. We can extract the leaves of the *Moringa oleifera* plant in this way to produce ZnONPs on a big scale. By using SEM and XRD measurements, it was demonstrated that ZnO nanoparticles had formed. The synthesized nanoparticles catalyze decolonization by actively destroying the Congo Red and Titan Yellow dye solutions in visible light illumination. The antibacterial properties of the synthesized ZnO-NPs were evaluated at deficient concentrations against harmful microorganisms such as *Bacillus subtilis* and *E. coli*. Considering all of the criteria

mentioned, it can be concluded that this method is a practical approach for nanoparticle production.

## References

- Ahmed S. and Ikram S. (2016). Biosynthesis of gold nanoparticles: A green approach, *Journal of Photochemistry and Photobiology B: Biology*, **161**, 141–153.
- Arviso R.R., Bhattacharyya S., Kudgus R.A., Giri K., Bhattacharya, R. and Mukherjee P. (2012). Intrinsic therapeutic applications of noble metal nanoparticles: past, present and future, *Chemical Society Reviews*, **41(7)**, 2943–2970.
- Azizi S., Ahmad M.B., Namvar F. and Mohamad R. (2014). Green biosynthesis and characterization of zinc oxide nanoparticles using brown marine macroalgae *Sargassum muticum* aqueous extract, *Materials Letters*, **116**, 275–277.
- Banerjee P., Satapathy M. and Mukhopahayay A. (2014). Green synthesis of silver nanoparticles using the leaf extract of *Pongamia pinnata* and evaluation of their antimicrobial activities, *Journal of Nanotechnology*, 2014.
- Bar H., Bhui D.K., Sahoo G.P., Sarkar P., Pyne S., and Misra A. (2009). Green synthesis of silver nanoparticles using seed extract of *Jatropha curcas*, *Colloids and Surfaces A: Physicochemical and Engineering Aspects*, **348(1–3)**, 212–216.
- Basnet P., Roy B., and Tako M. (2015). Green synthesis and characterization of silver nanoparticles using alcoholic flower extract of *Nyctanthes arbortristis* and in vitro investigation of their antibacterial activity, *Materials Letters*, **138**, 251–254.
- Bhuyar P., and Ganeshan V. (2017). Green synthesis of zinc oxide nanoparticles using *Moringa oleifera* leaf extract for degradation of dyes and antimicrobial activity, *Journal of Environmental Chemical Engineering*, **5(6)**, 6057–6066.
- Bindhu M.R., and Umadevi M. (2014). Synthesis of monodispersed silver nanoparticles using *Hibiscus cannabinus* leaf extract and its antimicrobial activity, *Spectrochimica Acta Part A: Molecular and Biomolecular Spectroscopy*, **121**, 164–167.
- Das R.K., Gogoi N., Bora U., and Dolui S.K. (2009). Green synthesis of gold nanoparticles using *Nyctanthes arbortristis* flower extract, *Bioprocess and Biosystems Engineering*, **32(6)**, 791–797.
- El-Rafie H.M., El-Rafie M.H., Zahran M.K. and El-Sakhawy M. (2012). Preparation and properties of carboxymethyl cellulose/cellulose acetate biodegradable blends, *Carbohydrate Polymers*, **89(2)**, 461–466.
- Firdhouse M.J. and Lalitha, P. (2015). Green synthesis of silver nanoparticles using the aqueous extract of the leaf of *Solanum nigrum* L. and its antimicrobial activity, *International Journal of Pharmaceutical Sciences Review and Research*, **31(1)**, 94–100.
- Geethalakshmi R. and Sarada D.V. (2010). Gold and silver nanoparticles from *Trianthema decandra*: Synthesis, characterization, and antimicrobial properties, *International Journal of Nanomedicine*, **5**, 753–762.
- Gopinath V., MubarakAli D., Priyadarshini S., Priyadarshini N.M., Thajuddin N. and Velusamy P. (2012). Biosynthesis of silver nanoparticles from *Tribulus terrestris* and its antimicrobial activity: A novel biological approach, *Colloids and Surfaces B: Biointerfaces*, **96**, 69–74.
- Huang J., Li Q., Sun D., Lu Y., Su Y., Yang X. and Wang H. (2007). Biosynthesis of silver and gold nanoparticles by novel sundried *Cinnamomum camphora* leaf, *Nanotechnology*, **18(10)**, 105104.
- Jha A.K., Prasad K. and Prasad K. (2009). A green low-cost biosynthesis of Sb<sub>2</sub>O<sub>3</sub> nanoparticles, *Biochemical Engineering Journal*, **43(3)**, 303–306.
- Khatoun N. and Mollah M.Y.A. (2016). Green synthesis of ZnO nanoparticles using *Psidium guajava* leaves extract and their characterization, *Journal of Materials Science: Materials in Electronics*, **27(11)**, 12122–12128.
- Kim S.W., Kim K.S., Lamsal K., Kim Y.J., Kim S.B., Jung M. and Lee Y.S. (2009). An in vitro study of the antifungal effect of silver nanoparticles on oak wilt pathogen *Raffaelea* sp, *Journal of Microbiology and Biotechnology*, **19(8)**, 760–764.
- Mahendra C. and Vinay S.P. (2014). Green synthesis of iron nanoparticles using *Artocarpus heterophyllus* leaf extract, *Journal of Chemical and Pharmaceutical Research*, **6(8)**, 1804–1807.
- Mittal A.K., Chisti Y. and Banerjee U.C. (2013). Synthesis of metallic nanoparticles using plant extracts, *Biotechnology Advances*, **31(2)**, 346–356.
- Nadagouda M.N., and Varma R.S. (2008). Green synthesis of silver and palladium nanoparticles at room temperature using coffee and tea extract, *Green Chemistry*, **10(8)**, 859–862.
- Nanda A. and Saravanan M. (2009). Biosynthesis of silver nanoparticles from *Staphylococcus aureus* and its antimicrobial activity against MRSA and MRSE, *Nanomedicine: Nanotechnology, Biology and Medicine*, **5(4)**, 452–456.
- Oves M., Khan M.S., Zaidi A. and Ahmed A.S. (2013). Ahmed, S., and Ikram, S. (2016). Silver nanoparticles: biosynthesis and antimicrobial potential, In *Microbial Applications 2: Biomedicine, Agriculture and Industry*, 25–36, Springer.
- Rajakumar G. and Rahuman A.A. (2011). Larvicidal activity of synthesized silver nanoparticles using *Eclipta prostrata* leaf extract against filariasis and malaria vectors, *Acta Tropica*, **118(3)**, 196–203.
- Rajiv P., Rajeshwari S., Venkatesh R. and Anand, S. (2013). Green synthesis of zinc oxide nanoparticles using *Atalantia monophylla* leaf extracts: Characterization and antimicrobial activity, *Materials Science and Engineering: C*, **33(7)**, 4017–4026.
- Rajkumari J., Thangamani S., and Meenakshisundaram M. (2017). Synthesis of zinc oxide nanoparticles using plant leaf extract against urinary tract infection pathogen, *Resource-Efficient Technologies*, **3(4)**, 459–466.
- Rathi J.M., Sudhakar C. and Singh D. (2016). Green synthesis of zinc oxide nanoparticles from *Catharanthus roseus* (Vinca rosea) leaf extract and their photocatalytic activity, *Journal of Materials Science: Materials in Electronics*, **27(7)**, 6881–6889.
- Saifuddin N., Wong C.W. and Yasumira A.A.N. (2009). Rapid biosynthesis of silver nanoparticles using culture supernatant of bacteria with microwave irradiation, *E-Journal of Chemistry*, **6(1)**, 61–70.
- Sathishkumar M., Sneha K., Won S.W., Cho, C.W., Kim, S., and Yun, Y.S. (2009). Cinnamon zeylanicum bark extract and powder mediated green synthesis of nano-crystalline silver particles and its bactericidal activity, *Colloids and Surfaces B: Biointerfaces*, **73(2)**, 332–338.
- Shankar S.S., Rai A., Ahmad A., and Sastry M. (2004). Rapid synthesis of Au, Ag, and bimetallic Au core-Ag shell nanoparticles using Neem (*Azadirachta indica*) leaf broth, *Journal of Colloid and Interface Science*, **275(2)**, 496–502.

- Shankar S.S., Rai A., Ankamwar B., Singh A., Ahmad A. and Sastry, M. (2004). Biological synthesis of triangular gold nanoprisms, *Nature Materials*, **3**(7), 482–488.
- Sharma V., Sharma P. and Sharma, A. (2019). Green synthesis of ZnO nanoparticles using *Moringa oleifera* leaf extract and their application in photocatalytic degradation of organic dyes, *Journal of Materials Science: Materials in Electronics*, **30**(6), 5700–5707.
- Shukla A.K., Iravani S. and Varma R.S. (2019). Green synthesis, characterization and applications of metal and metal oxide nanoparticles, In *Green Synthesis, Characterization and Applications of Nanoparticles*, 113–132, Elsevier.
- Singh P., Kim Y.J., Zhang D., Yang D.C. and Singh H. (2017). Biosynthesis, characterization, and antimicrobial applications of silver nanoparticles, *International Journal of Nanomedicine*, **12**, 2567–2577.
- Sudhakar C., Rathi J.M. and Singh, D. (2016). Green synthesis of zinc oxide nanoparticles from *Rosa indica* leaf extract and their photocatalytic activity, *Materials Letters*, **180**, 263–267.
- Suman T.Y., Radhika Rajasree S.R., Ramkumar R., Rajthilak C., Perumal P. and Rajasree S.R. (2015). Synthesis, characterization and evaluation of silver nanoparticles from *Sargassum plagiophyllum*: an economically important brown seaweed, *Bioprocess and Biosystems Engineering*, **3**(5), 961–969.
- Suresh D., Nethravathi P.C., Udayabhanu G., Rajanaika H. and Nagabhushana H. (2015). Microwave-assisted rapid green synthesis of silver nanoparticles using *Aloe barbadensis* miller gel and their antimicrobial studies, *Advances in Applied Science Research*, **6**(1), 165–172.
- Verma N. and Sharma S. (2016). Synthesis and applications of Au nanoparticles: An overview, *The Scientific World Journal*, 2015.
- Vijayakumar S., Vinoj G., Malaikozhundan B., Shanthy S. and Vaseeharan B. (2015). *Plectranthus amboinicus* leaf extract-mediated synthesis of zinc oxide nanoparticles and its control of methicillin-resistant *Staphylococcus aureus* biofilm and blood sucking mosquito larvae, *Spectrochimica Acta Part A: Molecular and Biomolecular Spectroscopy*, **137**, 886–891.
- Vivek R., Thangam R., Muthuchelian K. and Gunasekaran, P. (2012). Green biosynthesis of silver nanoparticles from *Annona squamosa* leaf extract and its in vitro cytotoxic effect on MCF-7 cells, *Process Biochemistry*, **47**(12), 2405–2410.